DEVELOPMENT OF A HYDRAULIC STIMULATION SIMULATOR TOOLBOX FOR ENHANCED GEOTHERMAL SYSTEM DESIGN

Sehyeok PARK[1], Kwang-Il KIM[1], Saeha KWON[1], Hwajung YOO[1], Linmao XIE[1], Ki-Bok MIN[1*], Kwang Yeom KIM[2]

[1]Seoul National University, 1, Gwanak-ro, Gwanak-gu, Seoul, 08826, Korea (Republic of)

[2]Korea Institute of Civil Engineering and Building Technology, 283, Goyang-daero, Ilsanseo-gu, Gyeonggi-do, 10223, Korea (Republic of)

*e-mail: kbmin@snu.ac.kr

ABSTRACT

Hydraulic stimulation is the key technology in the enhanced geothermal system (EGS) development. In this study, a reservoir stimulation simulator toolbox was developed for the comprehensive EGS design considering the natural fracture distribution, borehole stability, hydraulic stimulation and the thermal performance of the reservoir. The toolbox program consists of five modules, i.e., 3D discrete fracture network (DFN) generation, borehole stability analysis, hydrofracturing estimation, hydroshearing estimation and reservoir temperature prediction. Each module is implemented with graphic user interface using MATLAB® and available as a stand-alone program. The program allows independent analysis of each module and combined analyses with compatible data among the related modules, which provides extensive applicability to a variety of tasks associated with EGS stimulation, shale gas fracturing and CO2 geosequestration.

Keywords: enhanced geothermal system, hydrofracturing, hydroshearing, discrete fracture network, borehole stability, reservoir temperature

1. INTRODUCTION

Geothermal energy is the only renewable energy that can generate base load electricity. However, only the regions with high geothermal gradient and high reservoir permeability such as volcanic regions, had been preferred as a site for conventional geothermal power generation. Enhanced geothermal system (EGS) is being developed to achieve the geothermal power generation and direct heat use in non-volcanic regions with mid-to-high reservoir temperatures and low initial reservoir permeability (Tester et al., 2006).

In spite of the scientific achievements in many EGS projects over 40 years, EGS is still in the developmental stage and has many unresolved technical issues (Tester et al., 2006; Xie et al., 2015). First, new fractures must be properly created through hydrofracturing when natural fractures are not prevalent in the reservoir. Unlike in conventional oil and gas fields, this poses a unique challenge for hydrofracturing design in EGS due to the large distance between the wells. Second, when natural fractures already prevail in the reservoir, appropriate estimation of the hydroshearing behavior is critical because hydroshearing is

the main mechanism that increases the permeability of the fractured reservoir. Third, deep fractured reservoir has to be characterized and the knowledge of the discrete fracture network (DFN) is of special importance because the fractures will be the main conduits for fluid flow and heat convection. Fourth, deep drilling, as deep as 5 km, must be carried out safely and economically. Thus, the stability of such deep borehole is important for successful access to the deep target reservoir. Fifth, the thermal performance of the stimulated reservoir should be considered properly in the stimulation design to ensure economical and sustainable EGS applications.

Although many computer programs are being used for EGS designs, many of the cases are found as unsuccessful in terms of reflecting the unique characteristics of EGS reservoir. In this study, we present a hydraulic stimulation simulator toolbox which consists of five modules for hydrofracturing estimation, hydroshearing estimation, 3D DFN generation, borehole stability, and reservoir temperature prediction, many of which are often ignored or separately considered in each different program without a specific aim to the EGS stimulation design. We attempted to develop an all-in-one program tailored to support the swift technical decisions in EGS design by considering the previously mentioned five EGS designing issues and adopting EGS-specified estimation models that consider both hydrofracturing and hydroshearing as the stimulation mechanisms.

2. THEORIES

2.1. Analytic hydrofracturing models

For the implementation of hydrofracturing estimation module, two-dimensional analytic hydrofracturing models are reviewed and organized from previous studies (Economides and Nolte, 2000; Geertsma and De Klerk, 1969; Nordgren, 1972; Valko and Economides, 1995; Yew and Weng, 2014). There are largely three types of 2D hydrofracturing models distinguished by their fracture geometries, i.e., Perkins-Kern-Nordgren (PKN), Khristianovich-Geertsma-de Klerk (KGD) and KGD-based radial models (Fig. 1). The KGD and PKN models are the very basic hydrofracturing models for longitudinal fractures generated along the borehole, and these models can also be distinguished by the shape of vertical opening section. The radial fracture model is for transverse fracture that are perpendicular to the borehole. Actual calculation of the fracture dimensions or the fluid pressure is conducted with or without leak-off conditions on the fracture walls.

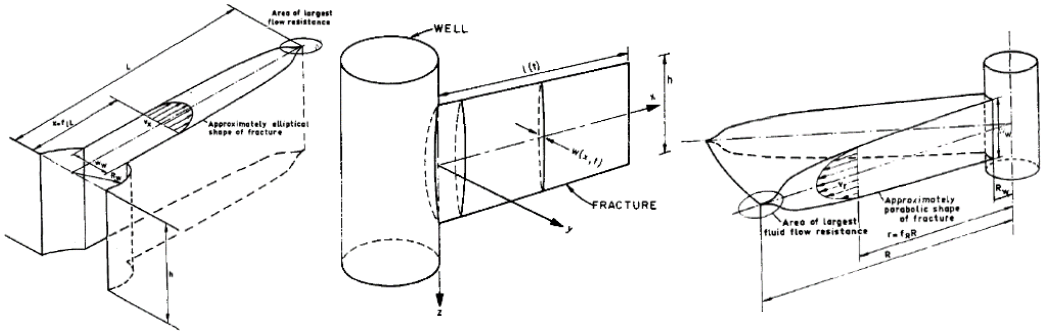

Fig. 1 Fracture geometries of the hydrofracturing models (Geertsma and De Klerk, 1969; Nordgren, 1972)

Table 1 Characteristics of 2D hydrofracturing models

Model	Plane strain direction	Overall shape	Aperture profile
KGD model	Horizontal	Vertical: long, horizontal: short	Vertical: rectangular, Horizontal: elliptic $w = w_w[1-(x/L)^2]^{1/2}$
PKN model	Vertical	Vertical: short, horizontal: long	Vertical: elliptic $w_z = w_x[1-(2z/h)^2]^{1/2}$, Horizontal: $w_x = w_w[1-x/L]^{1/4}$
Radial model	Vertical	Circular, Perpendicular to borehole	Parabolic $w = w_w[1-x/L]^{1/2}$

There are total six different types of calculations for three models, and commonly these calculations give fracture length L, aperture w and fluid pressure inside the fracture p as function of the injection time t, under given injection conditions and reservoir parameters. Eq. (1) – (6) are examples for KGD model cases:

1) KGD model with assumption of no leak-off: explicit form

$$\mathrm{L(t)} = 0.38\left[\frac{EQ^3}{(1-\nu^2)\mu h^3}\right]^{1/6} t^{2/3} \tag{1}$$

$$\mathrm{w}_w\mathrm{(t)} = 1.67\left[\frac{(1-\nu^2)\mu Q^3}{Eh^3}\right]^{1/6} t^{1/3}, \qquad \bar{w} = \frac{\pi}{4}\mathrm{w}_w \tag{2}$$

$$p_w\mathrm{(t)} = S + 1.09\left[\frac{\mu E^2}{(1-\nu^2)^2}\right]^{1/3} t^{-1/3} \tag{3}$$

2) KGD model with Carter's leak-off equations: implicit form

$$\mathrm{w}_{w,max} = 2.708\left[\frac{(1-\nu^2)\mu Q L^2}{hE}\right]^{1/4}, \qquad \bar{w} = \frac{\pi}{4}\mathrm{w}_{w,max} \tag{4}$$

$$\mathrm{L} = \frac{(\pi w_w + 8S_p)Q}{32C^2\pi h}\left[\exp(\alpha^2)\,erfc(\alpha) + \frac{2\alpha}{\sqrt{\pi}} - 1\right], \qquad \alpha = \frac{8C\sqrt{\pi t}}{\pi w_w + 8S_p} \tag{5}$$

Then the root-finding method is used to determine the consistent set of $\bar{w}$ and L at certain t, resulting in:

$$p_w = S + \frac{E}{4(1-\nu^2)L}\mathrm{w}_{w,max} \tag{6}$$

where t is the fluid injection time, L is the half-wing length of the longitudinal fracture, E is the Young's modulus of rock, ν is the Poisson's ratio of rock, Q is the constant volumetric flow rate into the borehole, μ is the fluid viscosity, h is the constant fracture height, w_w is the maximum fracture width at the boreshole wall, $\bar{w}$ is the average fracture width within the fracture, p_w is the net fluid pressure inside the fracture, S is the minimum principal stress, S_p is the spurt loss coefficient, and C is the leak-off coefficient.

2.2. Hydroshearing estimation model

Fracture shearing due to injected fluid pressure is implemented in the hydroshearing estimation module. Slip tendency is defined as the ratio of resolved shear stress to resolved normal stress acting on a fracture plane (Morris et al., 1996). In this study, the extended version of the slip tendency method developed by Xie and Min (2016) is used to implement it into the hydroshearing estimation module.

When the maximum, intermediate, and minimum in-situ principal stresses are given as σ_1, σ_2, and σ_3, respectively, the critical fluid pressure P_c for shearing a specific fracture can be calculated using Eq. (7) with the resolved shear stress τ and normal stress σ acting on the fracture plane:

$$P_c = \sigma - \tau/tan\phi \tag{7}$$

$$\tau = \sqrt{(\sigma_1-\sigma_2)^2 l^2 m^2 + (\sigma_2-\sigma_3)^2 m^2 n^2 + (\sigma_3-\sigma_1)^2 n^2 l^2} \tag{8}$$

$$\sigma = l^2\sigma_1 + m^2\sigma_2 + n^2\sigma_3 \tag{9}$$

where l, m, and n are direction cosines of the fracture plane normal to the principal stress axes, i.e., σ_1, σ_2, and σ_3, respectively.

The minimum critical fluid pressure P_{cm} for shearing an optimally-oriented fracture is calculated using the fracture friction angle ϕ using Eq. (10).

$$P_{cm} = \frac{k_c - k}{k_c - 1}\sigma_3, \qquad k = \frac{\sigma_1}{\sigma_3}, \qquad k_c = \frac{1+sin\phi}{1-sin\phi} \tag{10}$$

If the magnitudes of the in-situ stresses are assumed to be increasing linearly along with depth, the location of shearing onset within the open hole section and the direction of shearing migration can be estimated using the depth gradient of critical pressure (dP_c/dz):

$$\sigma_1 = k_1\sigma_v, \qquad \sigma_2 = k_2\sigma_v, \qquad \sigma_3 = k_3\sigma_v \tag{11}$$

$$d\sigma/dz = (l^2k_1 + m^2k_2 + n^2k_3)\rho_r g = \rho_\sigma g \tag{12}$$

$$d\tau/dz = \sqrt{(k_1-k_2)^2 l^2 m^2 + (k_2-k_3)^2 m^2 n^2 + (k_3-k_1)^2 n^2 l^2}\,\rho_r g = \rho_\tau g \tag{13}$$

$$dP_c/dz = \rho_\sigma g - \rho_\tau g/tan\phi = \rho_{pc} g \tag{14}$$

where ρ_r is the average density of the rock and g is gravitational acceleration. When ρ_{pc} is greater than the density of the injected fluid, the location of shearing initiation will be the casing shoe, and the shearing will migrate in the upward direction.

2.3. Statistical generation of 3D fracture network

In order to generate a fracture network, information on the fracture center location, orientation, size, aperture, and the total number of fractures should be given. The fracture parameters are assumed to be independent each other. Various probability distributions are used for each fracture parameters: 1) Fisher distribution for fracture orientation, 2) negative exponential and power law distributions for fracture length,

3) negative exponential, uniform random, normal, and log-normal distributions for fracture aperture (Priest, 1993). When a set of fracture parameters are given with corresponding probability distributions, a DFN can be generated by Monte-Carlo simulation using the pre-defined fracture parameters and probability distributions.

2.4. Stress concentration around a borehole in anisotropic rock

For the borehole stability module, both the analytic solution and the numerical method are used to estimate the stress concentration around a borehole, and the compressive and tensile failure regions are predicted using Mohr-Coulomb failure criterion and tensile strength, respectively. The generalized analytic solution of stress concentration around a cavity was derived by Lekhnitskii (1963). Starting from the general compatibility equation that can consider rock anisotropy, Airy stress function is derived and then every stress component throughout the model domain is calculated on an arbitrary point $z_k = r(cos\theta + \mu_k sin\theta)$. It requires the determination of the analytic function $\Phi_k(z_k)$, and it is derived as Eq. (15) for the case of general anisotropic elastic model with a single borehole (Ong, 1994):

$$\begin{aligned}
\Phi_1'(z_1) &= A_1\left[\begin{matrix}\left(i\sigma_{xy,o} - \sigma_{yy,o} + P_w\right)(\mu_2 - \lambda_2\lambda_3\mu_3) + \\ \left(\sigma_{xy,o} - i\sigma_{xx,o} + iP_w\right)(\lambda_2\lambda_3 - 1) + \left(\sigma_{yz,o} - i\sigma_{xz,o}\right)\lambda_3(\mu_3 - \mu_2)\end{matrix}\right] \\
\Phi_2'(z_1) &= A_2\left[\begin{matrix}\left(i\sigma_{xy,o} - \sigma_{yy,o} + P_w\right)(\lambda_1\lambda_3\mu_3 - \mu_1) + \\ \left(\sigma_{xy,o} - i\sigma_{xx,o} + iP_w\right)(1 - \lambda_1\lambda_3) + \left(\sigma_{yz,o} - i\sigma_{xz,o}\right)\lambda_3(\mu_1 - \mu_3)\end{matrix}\right] \\
\Phi_3'(z_1) &= A_3\left[\begin{matrix}\left(i\sigma_{xy,o} - \sigma_{yy,o} + P_w\right)(\mu_1\lambda_2 - \mu_2\lambda_1) + \\ \left(\sigma_{xy,o} - i\sigma_{xx,o} + iP_w\right)(\lambda_1 - \lambda_2) + \left(\sigma_{yz,o} - i\sigma_{xz,o}\right)(\mu_2 - \mu_1)\end{matrix}\right] \\
\mathrm{A_k} &= 1/2 * \left[[\mu_2 - \mu_1 + \lambda_3\lambda_2(\mu_1 - \mu_3) + \lambda_1\lambda_3(\mu_3 - \mu_2)]\zeta_k\sqrt{(z_k/a)^2 - 1 - \mu_k^2}\right]^{-1}
\end{aligned} \tag{15}$$

where P_w is the fluid pressure applied on the borehole wall, ζ_k is a constant for the transformation of coordinate z_k, and a is the borehole radius, σ_{ij} is the calculated local stress at specific coordinates, $\sigma_{ij,o}$ is the far field stress, μ_k is the root of the characteristic equation, and λ_k is the constant derived from the characteristic equation.

The analytic solution gives rapid calculation results for a simple, pre-defined model, but it has limited applicability to complex model geometry, physical properties, and boundary conditions. Thus, the numerical computation option using the 2D finite element method (FEM) was implemented also in the borehole stability module. FEM simulation can provide a good reference results comparable to the analytic solution.

2.5 Analytic models on geothermal reservoir temperature

Under the assumptions of impermeable isotropic rock and several parallel uniform-spacing fractures which act as the flow path, the spatial temperature distribution within the reservoir and geothermal fluid can be calculated at the circulation time t with three analytical models below (Bodvarsson, 1969; Gringarten et al., 1975; Bödvarsson and Tsang, 1982):

Single fracture, rectilinear flow:

$$T(x,\ z,\ t) = T_{ro} + (T_{wo} - T_{ro})erfc\left[\frac{\alpha x + z}{2\sqrt{at}}\right], \qquad \alpha = \frac{2kNW}{c_w Q} \tag{16}$$

Multiple parallel fractures with uniform spacing, rectilinear flow:

$$T_D(x_D,\ z_D,\ s) = \frac{1}{s} exp\left[-x_D\sqrt{s} * tanh\left(\beta D_{ED}\sqrt{s}\right)\right] * \left[cosh\left(\beta z_D\sqrt{s}\right) - tanh\left(\beta D_{ED}\sqrt{s}\right)sinh\left(\beta z_D\sqrt{s}\right)\right], \qquad \beta = \frac{c_w Q}{2kHNW} \tag{17}$$

Multiple parallel fractures with uniform spacing, radial flow:

$$T_D(\xi,\ \eta,\ p) = \frac{1}{p} exp\left(-\frac{2\sqrt{p}\tanh\left(\sqrt{p}\right)}{2+\theta}\xi\right) * \left[cosh\left(\sqrt{p}\eta\right) - sinh\left(\sqrt{p}\eta\right)tanh\left(\sqrt{p}\right)\right], \tag{18}$$

$$\xi = \frac{Nk\pi r^2(2+\theta)}{c_w Q D}, \qquad \theta = \frac{\rho_w c_w b}{\rho_r c_r D}, \qquad \eta = \frac{z}{D}$$

where x is the distance from the injection point, z is depth into the rock matrix measured perpendicular to the fracture plane, T_{ro} is the initial reservoir temperature, T_{wo} is the fluid injection temperature, a is the thermal diffusivity of rock, k is the thermal conductivity of rock, N is the number of fractures, W is the fracture width in the y direction (Fig 2), Q is total mass flow rate in the borehole, T_D is the Laplace transform of dimensionless temperature, x_D is dimensionless x, z_D is dimensionless z, s and p are the Laplace parameters, D is half-spacing of the fractures, D_{ED} is dimensionless D, b and H are arbitrary values for dimensionless forms, r is the distance from the injection point along the radial flow direction, ξ is dimensionless r, θ is dimensionless energy potential, η is dimensionless z in the radial flow, ρ_w is fluid density, ρ_r is rock density, c_w is the specific heat of the fluid, and c_r is the specific heat of rock.

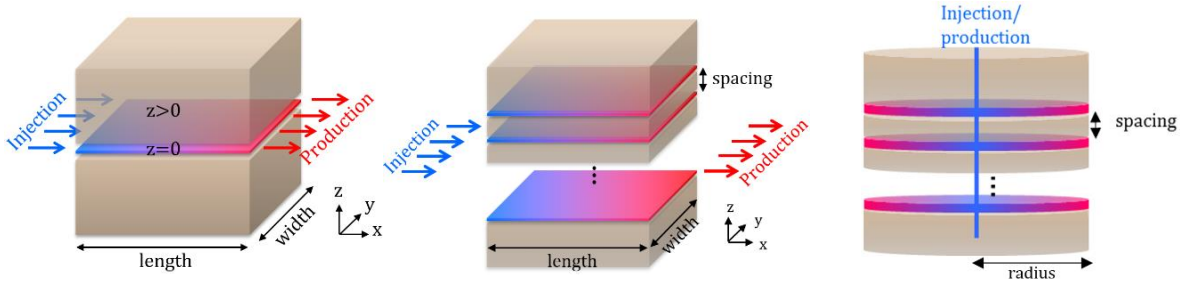

Fig. 1 Schematic diagrams of the geometries of geothermal reservoir temperature models

3. PROGRAM IMPLEMENTATIONS

Based on the theoretical models introduced in section 2, five program modules were developed using MATLAB® technical computing language: 1) hydrofracturing estimation module, 2) hydroshearing estimation module, 3) 3D DFN generation module, 4) borehole stability module, and 5) reservoir temperature prediction module. Each module can be operated as an independent program, and it also supports combined analyses such as hydrofracturing-thermal simulation and 3D DFN-hydroshearing simulation, thanks to the full compatibilities of the data among the related modules.

3.1. Hydrofracturing estimation & reservoir temperature prediction

The hydrofracturing estimation module can provide the estimates on the generated fracture shapes and dimensions and fluid pressure within the fracture under certain input conditions on reservoir and fluid injection properties. The reservoir temperature prediction module can give predictions on the geothermal reservoir temperature distributions in space and its change in time under given input parameters on reservoir properties, injection conditions and fracture set geometries.

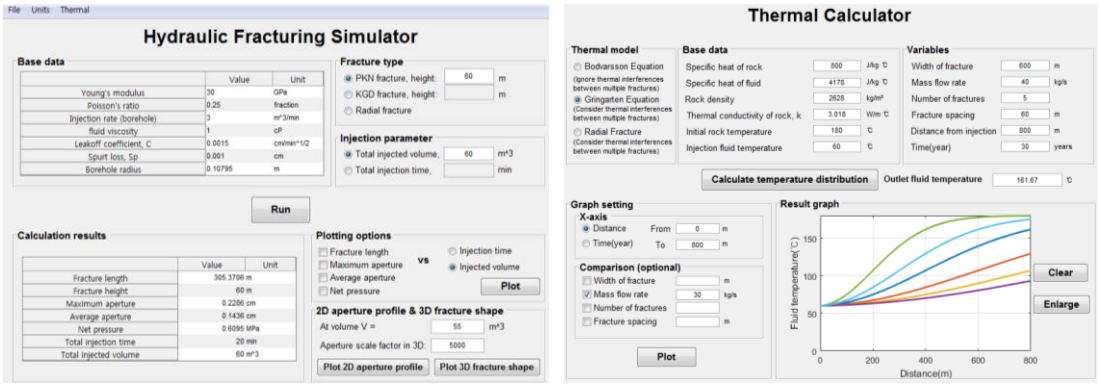

Fig. 3 GUIs of (left) Hydrofracturing estimation module and (right) temperature prediction module

User can also run these two simulators in combined manner. Under the assumption of very small aperture, the fracture geometries of the PKN and KGD models can be directly adopted into the reservoir temperature models with rectilinear flow. For radial hydrofracturing model also, its geometry can be directly adopted into the radial flow temperature model. In consequence, it is possible to run a geothermal reservoir temperature prediction based on the fracture geometries calculated by hydrofracturing simulation module. The combined hydrofracturing-temperature analysis can be applied for effective design of multi-stage hydrofracturing considering the long-term thermal performance of the reservoir.

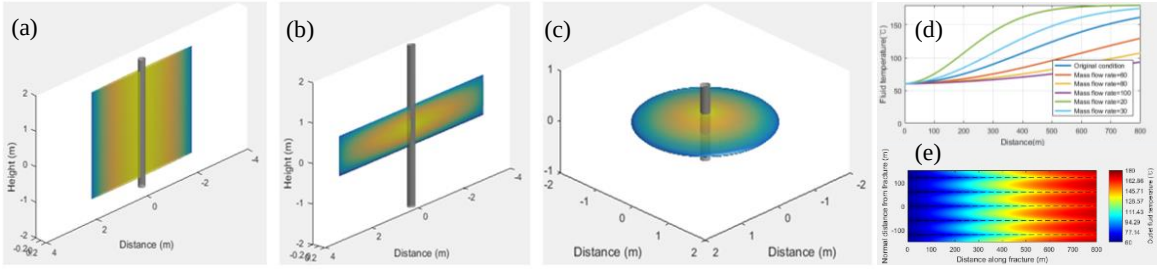

Fig. 4 (a) – (c) 3D visualizations of KGD, PKN and radial fractures, respectively; (d) spatial temperature profile with different flow rates; (e) temperature distribution within multiple parallel fracture system

3.2. 3D DFN generation & hydroshearing estimation

Using the Monte-Carlo simulation method, the 3D DFN generation module can generate a 3D DFN with its fracture parameters following the probability distributions of each own. The hydroshearing estimation

module can provide the estimates on the required fluid pressure, optimal orientation, initiation location and migration direction of the hydroshearing under given in-situ stress conditions and joint orientations.

One limitation of hydroshearing estimation module is that its prediction of optimal hydroshearing orientation and corresponding minimum critical pressure are assuming densely and uniform-randomly distributed natural fracture orientations, which cannot be always true in real reservoir situation. In this regard, two unique functions were implemented in the modules; first, 3D DFN generation module supports the extraction of the location and orientation data of borehole-intersecting fractures from the generated 3D DFN. Hydroshearing estimation module also supports the data import of borehole-intersecting DFN fractures into the hydroshearing simulation. As a consequence, the reliability of hydroshearing estimation is upgraded by using the Monte-Carlo-simulated 3D DFN data which is statistically identical to the target fracture network of in-situ reservoir. The DFN-combined hydroshearing estimation can be applied for effective design of hydroshearing-dominant stimulation in fractured geothermal reservoir.

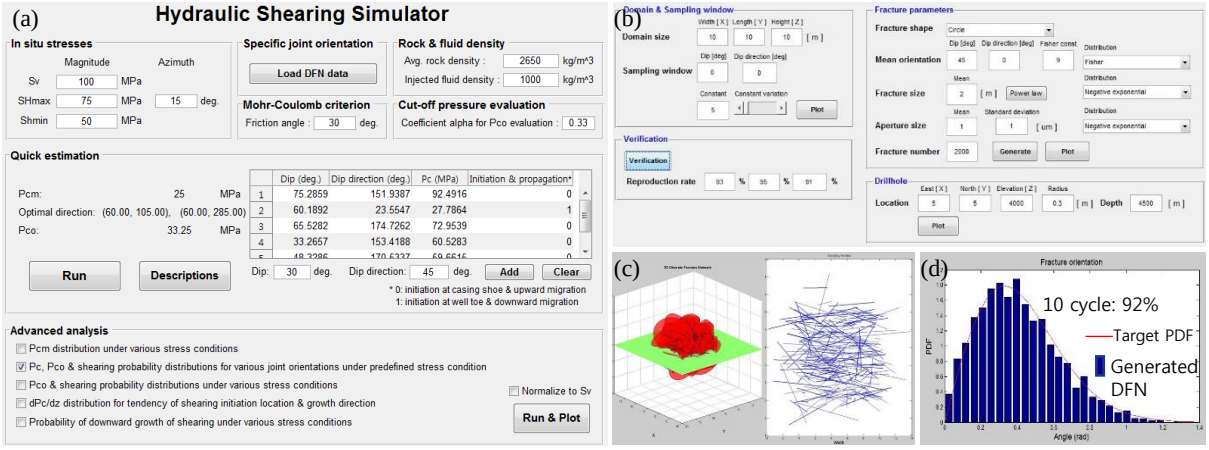

Fig. 5 (a), (b) Main GUIs of hydroshearing simulation and 3D DFN generation modules, respectively; (c) generation of 3D DFN and its traces on a sampling window; (d) comparison of the targeted probability distribution and Monte-Carlo-simulated DFN distribution

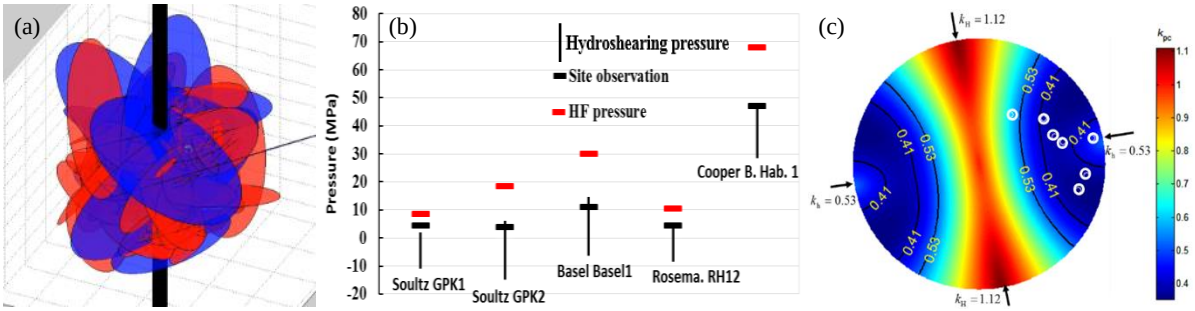

Fig. 6 (a) Automatic detection of borehole-intersecting fractures in DFN generation module; (b) comparison of estimated hydroshearing pressure and site observations; (c) comparison of observed fracture zone (white dots) and estimated optimal shearing zone (blue) in Soultz (Xie and Min, 2016)

3.3. Borehole stability analysis considering the well trajectory and rock anisotropy

One of the advantages of this module is that it is capable of borehole stability analyses for a borehole in a transversely isotropic rock. The module also considers the borehole inclination, thermal stress, and injection pressure, which expands the applicability of this module to various field cases.

The developed borehole stability analysis module supports various display options of stresses along a line, in a domain, or as the Mohr circles. The compressive and tensile failure regions around the borehole also can be indicated on the contour graph by enabling the failure criteria option and designating specific values for uniaxial compressive strength, friction angle, and tensile strength.

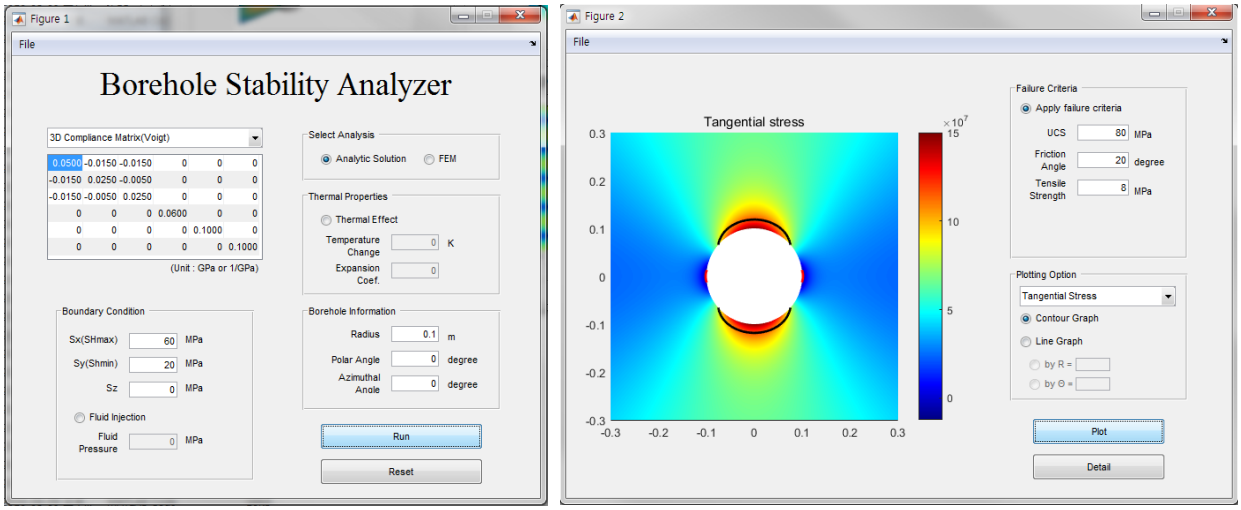

Fig. 5 GUIs of (left) Hydrofracturing estimation module and (right) temperature prediction module

4. CONCLUSIONS

- We presented a reservoir stimulation simulator toolbox program composed of five modules. 1) The hydrofracturing estimation module can provide estimates of the generated fracture shapes, fracture dimensions, and net fluid pressure within the fracture with a given set of input conditions on the reservoir and fluid injection properties. 2) The hydroshearing estimation module provides the estimates of the fluid pressure required for hydroshearing, the optimal orientation of hydroshearing, the hydroshearing initiation location and migration direction for the given in-situ stress conditions and fracture orientations. 3) Using the Monte-Carlo simulation method, the 3D DFN generation module can generate three-dimensional DFN with its fracture parameters following the probability distributions. 4) The borehole stability module can be used to analyze the stress concentrations around a borehole considering the rock anisotropy and the borehole trajectory, and it also can predict the compressive and tensile failure regions near the borehole. 5) The reservoir temperature prediction module can predict the temperature distributions within the fluid-circulating parallel fracture system and the corresponding distributions of the produced fluid temperature, so it can address the requirements the circulation system for sufficient production temperature and long-term sustainability considering the reservoir thermal drawdown.
- While the five modules can be used independently, they also can be used for combined studies, such

as hydrofracturing-temperature estimation analysis or 3D DFN-hydroshearing estimation for more effective estimation for EGS stimulation design.

- Because of similarities in the physical processes associated with EGS stimulation, each individual module also can be used to study several geo-environmental issues such as carbon capture and sequestration, hydrofracturing for shale gas development, and high-level nuclear waste repositories.

ACKNOWLEDGEMENT

This work was supported by the Korea Institute of Energy Technology Evaluation and Planning (KETEP) granted financial resource from the Ministry of Trade, Industry & Energy, Republic of Korea (No. 20133030000240).

REFERENCES

Bodvarsson, G. (1969): On the temperature of water flowing through fractures, *Journal of Geophysical Research*, **74 (8),** 1987-1992

Bodvarsson, G.S. and Tsang, C.F. (1982): Injection and thermal breakthrough in fractured geothermal reservoirs, *Journal of Geophysical Research: Solid Earth*, **87(B2),** 1031-1048

Economides, M.J., Nolte, K.G. (2000): Reservoir stimulation, 3rd edition, Wiley, Chichester.

Geertsma, J., De Klerk, F. (1969): A rapid method of predicting width and extent of hydraulically induced fractures, *Journal of Petroleum Technology*, **21(12)**, 1-571

Gringarten, A.C., Witherspoon, P.A., Ohnishi, Y. (1975): Theory of heat extraction from fractured hot dry rock, *Journal of Geophysical Research*, **80(8),** 1120-1124

Lekhnitskii, S.G. (1963): Theory of Elasticity of an Anisotropic Elastic Body, 1st edition, Holden-Day, Inc. San Francisco, California.

Morris, A., Ferrill, D.A., Henderson, D.B. (1996): Slip-tendency analysis and fault reactivation, *Geology*, **24(3)**, 275-278

Nordgren, R.P. (1972): Propagation of a vertical hydraulic fracture. *Society of Petroleum Engineers Journal*, **12(04)**, 306-314

Ong, S.H. (1994): Borehole Stability. Ph.D. Dissertation, University of Oklahoma, Oklahoma

Priest, S.D. (1993): Discontinuity analysis for rock engineering, Springer Science & Business Media.

Tester, J.W., et al. (2006): The Future of Geothermal Energy: Impact of Enhanced Geothermal Systems (EGS) on the United States in the 21st Century, Massachusetts Institute of Technology, Cambridge, Massachusetts.

Valko, P., Economides, M.J. (1995): Hydraulic fracture mechanics, 1st edition, Wiley, New York

Xie, L., Min, K.B., Song, Y. (2015): Observations of hydraulic stimulations in seven enhanced geothermal system projects, *Renewable Energy*, **79**, 56-65

Xie, L. and Min, K.B. (2016): Initiation and propagation of fracture shearing during hydraulic stimulation in enhanced geothermal system, *Geothermics*, **59**, 107-120

Yew, C.H. and Weng, X. (2014): Mechanics of hydraulic fracturing, 2nd edition, Gulf Professional Publishing.